

J/ψ suppression at $\sqrt{s} = 200$ GeV in the comovers' interaction model

A. Capella¹, E.G. Ferreira^{2,a}

¹ Laboratoire de Physique Théorique*, Université de Paris XI, Bâtiment 210, 91405 Orsay Cedex, France

² Departamento de Física de Partículas, Universidade de Santiago de Compostela, 15782 Santiago de Compostela, Spain

Received: 9 May 2005 /

Published online: 27 July 2005 – © Springer-Verlag / Società Italiana di Fisica 2005

Abstract. The yield of J/ψ per binary nucleon–nucleon collision in AuAu and CuCu collisions at $\sqrt{s} = 200$ GeV is computed in the framework of the dual parton model, supplemented with final state interaction (comovers' interaction). For the latter we use the same value of the cross-section, $\sigma_{co} = 0.65$ mb, which describes the anomalous J/ψ suppression observed at CERN-SPS energies. Several possibilities for the value of the absorptive cross-section are considered. Shadowing is introduced in both the comovers' and the J/ψ yields. A comparison with the results at CERN-SPS, including a prediction for InIn collisions, is also presented.

1 Introduction

J/ψ production in proton–nucleus collisions is suppressed with respect to the characteristic A^1 scaling of lepton pair production (Drell–Yan pairs). This suppression is generally interpreted as a result of the multiple scattering of a pre-resonance $c\bar{c}$ with the nucleons of the nucleus (nuclear absorption). In these interactions, the $c\bar{c}$ pair can transform into another $c\bar{c}$ pair with vanishing projection into J/ψ . The corresponding cross-section σ_{abs} is called the absorptive cross-section. This interaction is generally described in the framework of a probabilistic Glauber model. However, at high energies, the coherence length increases and the projectile interacts with the nucleus as a whole. As a consequence the probabilistic Glauber formula breaks down [1, 2] and, thus, the extrapolation from CERN-SPS energies to RHIC ones ($\sqrt{s} = 200$ GeV) is not straightforward.

The NA50 Collaboration has observed [3] the existence of anomalous J/ψ suppression in Pb–Pb collisions, i.e. the J/ψ suppression in central Pb–Pb collisions clearly exceeds the one expected from nuclear absorption. Such a phenomenon was actually predicted by Matsui and Satz [4] as a consequence of deconfinement in a dense medium. It can also be described as a result of a final state interaction of the $c\bar{c}$ pair with the dense medium produced in the collision (comovers' interaction). The final results [3] of the NA50 Collaboration can be described using an effective cross-section $\sigma_{co} = 0.65$ mb [5]. Since this is a low energy cross-section it is not expected to change significantly in going from CERN-SPS to RHIC energies. Therefore the

prediction of the J/ψ suppression due to comovers' interaction at RHIC seems to be quite safe. However, at these energies it is necessary to introduce shadowing corrections. These are small at CERN-SPS energies. Moreover, they cancel to a large extent in the ratio of J/ψ over Drell–Yan pair production measured by NA50. At RHIC energies, however, the Drell–Yan pair production is not measured and the J/ψ suppression is presented as a ratio of the J/ψ yield over the average number of binary nucleon–nucleon collisions – where the effect of shadowing is clearly present.

2 The model

The ratio $R_{AB}^{J/\psi}(b)$ of the J/ψ yield over the average number of binary nucleon–nucleon collisions, $n(b)$, in AB collisions is given by

$$R_{AB}^{J/\psi}(b) = \frac{dN_{AB}^{J/\psi}(b)/dy}{n(b)} \quad (1)$$
$$= dN_{pp}^{J/\psi}/dy \frac{\int d^2s \sigma_{AB}(b)n(b,s)S^{abs}(b,s)S^{co}(b,s)}{\int d^2s \sigma_{AB}(b)n(b,s)}.$$

Here $\sigma_{AB}(b) = 1 - \exp[-\sigma_{pp}ABT_{AB}(b)]$ where $T_{AB}(b) = \int d^2s T_A(s)T_B(b-s)$ and $T_A(b)$ is the profile function obtained from Wood–Saxon nuclear densities [6], and

$$n(b,s) = AB\sigma_{pp}T_A(s)T_B(b-s)/\sigma_{AB}(b). \quad (2)$$

^a e-mail: elena@fpaxp1.usc.es

* Unité Mixte de Recherche UMR no. 8627 - CNRS.

Upon integration of (2) over d^2s we obtain the average number $n(b)$ of binary nucleon–nucleon collisions at fixed impact parameter b .

The factors S^{abs} and S^{co} in (1) are the J/ψ survival probability due to nuclear absorption and comovers' interaction, respectively.

In writing (1) we have assumed that the J/ψ yield in the absence of final state interactions (i.e. $S^{\text{abs}} = S^{\text{co}} = 1$) scales with the number of binary nucleon–nucleon collisions. In this case $R_{AB}^{J/\psi}$ coincides with the J/ψ yield in pp collisions.

(a) Comovers interaction. The survival probability $S^{\text{co}}(b, s)$ of the J/ψ due to the comovers' interaction is obtained by solving the gain and loss differential equations which govern the final state interactions with the co-moving medium [7],

$$\tau \frac{dN^{J/\psi}(b, s, y)}{d\tau} = -\sigma_{\text{co}} N^{J/\psi}(b, s, y) N^{\text{co}}(b, s, y) \quad (3)$$

where $N^{J/\psi}$ and N^{co} are the densities (i.e. number per unit of transverse surface) of J/ψ and comovers (charged + neutral), respectively. In (3) we have neglected a gain term resulting from the recombination of c and \bar{c} into J/ψ . This is natural in our approach since the cross-sections for recombination (gain) are expected to be substantially smaller than σ_{co} . The possibility of such a recombination, giving sizable effects at RHIC energies, has been considered by several authors [8]. It will be most interesting to see whether the data confirm or reject such an effect.

In writing (3) we have neglected transverse expansion and assumed a dilution in time of the densities due to longitudinal motion which leads to a τ^{-1} dependence on proper time τ . Equation (3) can be solved analytically. The solution is invariant under the change $\tau \rightarrow c\tau$. Thus, the result depends only on the ratio τ_f/τ_0 of final over initial time. Using the inverse proportionality between proper time and densities, we put $\tau_f/\tau_0 = N^{\text{co}}(b, s, y)/N_{pp}(y)$, i.e. we assume that the interaction stops when the densities have diluted, reaching the value of the pp density at the same energy. At $\sqrt{s} = 200$ GeV and $y^* \sim 0$, $N_{pp}(0) = \frac{3}{2} (dN^{\text{ch}}/dy)_{y^*=0}^{pp} / \pi R_p^2 \sim 2.24 \text{ fm}^{-2}$. Note the increase in the pp density from 1.15 fm^{-2} at CERN-SPS to 2.24 fm^{-2} . Since the corresponding increase in the AuAu densities is approximately the same, the average value of τ_f/τ_0 is about the same at the two energies (of the order of $5 \div 7$).

The solution of (3) is given by [5]

$$S^{\text{co}}(b, s) \equiv N^{J/\psi(\text{final})}(b, s, y) / N^{J/\psi(\text{initial})}(b, s, y) \quad (4)$$

$$= \exp[-\sigma_{\text{co}} N^{\text{co}}(b, s, y) \ln(N^{\text{co}}(b, s, y)/N_{pp}(0))].$$

(b) Comovers density in the dual parton model. The main ingredient in order to compute the survival probability S^{co} is the comovers' density N^{co} . Note that N^{co} is the comovers' density at initial time τ_0 , i.e. the density produced in the primary collision. It can be computed in the dual parton model [9]. It can be seen from (6.1) of [9] that this density is given by a linear combination of the average number of participants and of binary nucleon–nucleon collisions, and

for $A = B$ can be written as

$$N_{\text{NS}}^{\text{co}}(b, s, y) = \frac{3}{2} \frac{dN_{\text{NS}}^{\text{ch}}}{dy}(b, s, y) \quad (5)$$

$$= \frac{3}{2} [C_1(b)n_A(b, s) + C_2(b)n(b, s)]$$

where

$$n_A(b, s) \quad (6)$$

$$= AT_A(s) [1 - \exp(-\sigma_{pp} u_B T_B(b - s))] / \sigma_{AB}(b)$$

and $n(b, s)$ is given by (2). The factor $3/2$ takes care of the neutrals. The coefficients $C_1(b)$ and $C_2(b)$ are obtained from string multiplicities which are computed in DPM as a convolution of momentum distributions functions and fragmentation functions. These functions are universal, i.e. the same for all hadronic and nuclear processes. Thus, we use the same expressions as at CERN energies. For details see [10]. The numerical values of $C_1(b)$ and $C_2(b)$ in AuAu and CuCu collisions at $\sqrt{s} = 200$ computed in the rapidity interval $|y^*| < 0.35$ for various values of b and per unit rapidity are given in Table 1. We also give in this table the corresponding values for PbPb and InIn at $p_{\text{lab}} = 158 \text{ GeV}/c$.

We see from Table 1 that C_2 is significantly larger than C_1 at RHIC energies. Thus, DPM leads to multiplicities which have a behavior closer to a scaling with the number of binary collisions rather than to a scaling with the number of participants. Actually, with increasing energies the ratio C_2/C_1 increases, and one obtains a scaling in the number of binary collisions. This is a general property of Gribov's reggeon field theory which is known as AGK cancellation [11] – analogous to the factorization theorem in perturbative QCD and valid for soft collisions in the absence of triple pomeron diagrams. It is well known that this behaviour is inconsistent with data which show a much smaller increase with centrality. As discussed in detail in [10] such a discrepancy is due to shadowing which is important at RHIC energies and has not been taken into account in (5). This is precisely the meaning of the label NS (no shadowing) in this equation.

(c) Shadowing. Following [10, 12, 13] shadowing corrections are computed, without free parameters, in terms of the measured value of the diffractive cross-section. Indeed, in the framework of Gribov's reggeon field theory, the same triple pomeron diagrams which describe high-mass diffraction are responsible for the shadowing corrections. While the contribution of the triple pomeron diagram to high-mass diffraction is positive, its contribution to the total cross-section is negative, due to the presence of s -channel discontinuities which correspond to interference terms. Thus, the triple pomeron diagrams (with triple pomeron coupling determined from high-mass diffraction data) produce a decrease of the charged yield as given by (5)–(7), thereby violating the AGK cancellation. In AB collisions this reduction is given¹ by [10, 12]

¹ A more sophisticated calculation using other triple Regge diagrams, with parameters constrained from HERA data can

Table 1. Values of C_1 and C_2 in (5) as a function of the impact parameter b . The second and third columns correspond to AuAu collisions and the fourth and fifth to CuCu collisions both at $\sqrt{s} = 200$ GeV. The values, calculated in the range $-0.35 < y^* < 0.35$, are given per unit rapidity. The following columns refer to PbPb and InIn at $p_{\text{lab}} = 158$ GeV/ c and are computed in the rapidity range of the NA50 dimuon trigger $0 < y^* < 1$

b	C_1 AuAu	C_2 AuAu	C_1 CuCu	C_2 CuCu	C_1 PbPb	C_2 PbPb	C_1 InIn	C_2 InIn
0.	1.0274	1.7183	1.0330	1.8196	0.7102	0.3975	0.7480	0.4312
1.	1.0276	1.7206	1.0334	1.8239	0.7115	0.3987	0.7485	0.4317
2.	1.0278	1.7228	1.0338	1.8320	0.7152	0.4020	0.7527	0.4357
3.	1.0286	1.7340	1.0342	1.8437	0.7208	0.4070	0.7599	0.4428
4.	1.0293	1.7448	1.0347	1.8592	0.7283	0.4136	0.7696	0.4526
5.	1.0302	1.7574	1.0352	1.8787	0.7376	0.4218	0.7810	0.4646
6.	1.0310	1.7722	1.0357	1.9014	0.7488	0.4320	0.7945	0.4793
7.	1.0320	1.7908	1.0361	1.9258	0.7617	0.4445	0.8112	0.4985
8.	1.0330	1.8121	1.0364	1.9505	0.7764	0.4597	0.8290	0.5198
9.	1.0340	1.8374	1.0364	1.9754	0.7929	0.4776	0.8475	0.5430
10.	1.0349	1.8665	1.0363	2.0006	0.8112	0.4985	0.8664	0.5681
11.	1.0357	1.8990	1.0360	2.0259	0.8308	0.5220	0.8855	0.5949
12.	1.0362	1.9308	1.0356	2.0515	0.8503	0.5466	0.9046	0.6235
13.	1.0364	1.9580	1.0349	2.0772	0.8673	0.5698	0.9233	0.6536

$$S_{\text{sh}}^h(b, s, y) = \frac{1}{1 + AF_h(y)T_A(s)} \frac{1}{1 + BF_h(y)T_B(b-s)}. \quad (7)$$

Here the function $F(y)$ is given by the integral of the ratio of the triple pomeron cross-section $d^2\sigma^{PPP}/dYdt$ at $t=0$ over the single pomeron exchange cross-section σ_P :

$$F_h(y) = 4\pi \int_{Y_{\text{min}}}^{Y_{\text{max}}} dY \frac{1}{\sigma_P} \frac{d^2\sigma^{PPP}}{dYdt} \Big|_{t=0} = C [\exp(\Delta Y_{\text{max}}) - \exp(\Delta Y_{\text{min}})], \quad (8)$$

where $Y_{\text{min}} = \ln(R_A m_N / \sqrt{3})$, $\Delta = 0.13$ and $C = 0.31 \text{ fm}^2$. The value of Y_{max} depends on the rapidity of the produced particle. For $y^* = 0$ we have $Y_{\text{max}} = 1/2 \ln(s/m_T^2)$ where m_T is the transverse mass of the produced particle. For charged particles we use $m_T = 0.4 \text{ GeV}$ and for a J/ψ $m_T = 3.1 \text{ GeV}$.

It has been shown in [10] that with the shadowing resulting from (7) and (8) a good description of the centrality dependence of charged multiplicities at mid-rapidities is obtained at RHIC energies ($\sqrt{s} = 130$ and 200 GeV). More precisely one has

$$N^{\text{co}}(b, s, y) = N_{\text{NS}}^{\text{co}}(b, s, y) S_{\text{sh}}^{\text{ch}}(b, s, y), \quad (9)$$

where the two factors in the RHS are given by (5) and (7), respectively.

With this expression of the density of comovers we can compute the J/ψ survival probability S^{co} , (4). The J/ψ suppression $R_{AB}^{J/\psi}$ is given by (1) with the following

be found in [13]. The results, however, are very similar to the ones obtained from (7) and (8).

replacement in its numerator:

$$n(b, s) \rightarrow n(b, s) S_{\text{sh}}^{J/\psi}(b, s, y). \quad (10)$$

Indeed, as discussed above, in writing the numerator of (1) we have assumed that the J/ψ yield in the absence of final state interactions ($S^{\text{abs}} = S^{\text{co}} = 0$) scales with the number of binary collisions. This is only true when shadowing is neglected. The effects of shadowing on the J/ψ yield are introduced with the replacement (10) in the numerator of (1).

(d) Nuclear absorption. The formula for nuclear absorption used in the literature is obtained in a probabilistic Glauber model. One has

$$S^{\text{abs}}(b, s) = \frac{[1 - \exp(-AT_A(s)\sigma_{\text{abs}})][1 - \exp(-BT_B(b-s)\sigma_{\text{abs}})]}{\sigma_{\text{abs}}^2 ABT_A(s)T_B(b-s)}. \quad (11)$$

As discussed in the Introduction, this formula breaks down at high energy due to the increase of the coherence length [1, 2]. In the limit of $s \rightarrow \infty$, the relevant equation is quite simple. The change consists in the replacement

$$(1/\sigma_{\text{abs}}) [1 - \exp(-\sigma_{\text{abs}} AT_A(b))] \Rightarrow AT_A(b) \exp\left[-\frac{1}{2} \sigma_{c\bar{c}-N} AT_A(b)\right] \quad (12)$$

in each of the two factors in the numerator of (11). The corresponding formula at finite energies which interpolates between (1) and (2) has also been derived [1]. The change in going from (11) to (12) is twofold. There is a change in the form of the expression and, moreover, σ_{abs} has been replaced by the total $c\bar{c}-N$ cross-section $\sigma_{c\bar{c}-N}$. If $\sigma_{c\bar{c}-N} \sim \sigma_{\text{abs}}$ the change from low energies to asymptotic

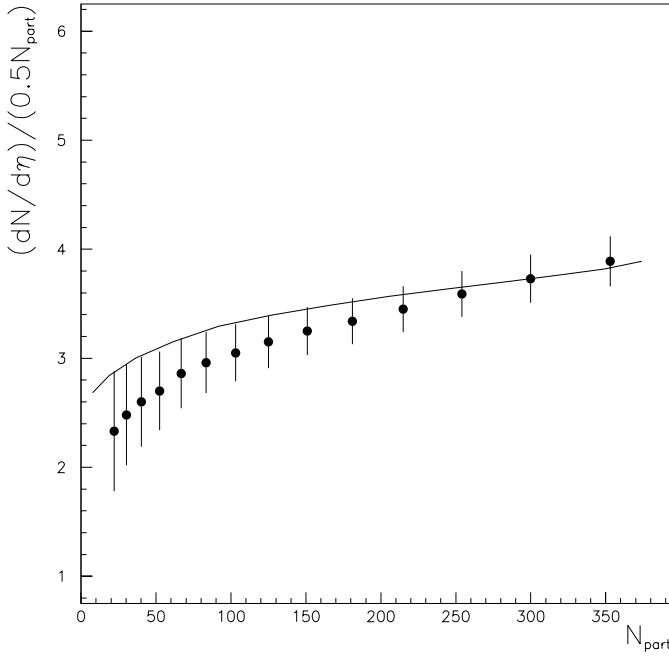


Fig. 1. Multiplicity of charged particles per participant pairs, versus N_{part} , computed from (13) are compared to experimental data from PHENIX [15]

ones is small. Indeed the two expressions coincide at the first and second order in the development of the exponential, and since σ_{abs} is small, the low energy result will not be significantly changed. However, if $\sigma_{c\bar{c}-N}$ is significantly larger than its absorptive part, σ_{abs} , the J/ψ suppression due to final state interaction within the nucleus will be larger at high energies. The latter possibility seems to be ruled out by preliminary data [14] on d Au collisions, which show a rather small suppression at mid-rapidities.

In the next section we present the calculation of J/ψ suppression in AuAu and CuCu collisions using (11) with the value $\sigma_{\text{abs}} = 4.5$ obtained from the pA data at CERN-SPS. With these values of σ_{abs} the results obtained with (1) and (2) are practically the same. We also present the results obtained with smaller values of σ_{abs} ($\sigma_{\text{abs}} = 0, 1$ mb and 3 mb).

3 Numerical results

We compute first the inclusive charged particle multiplicity given by

$$\frac{dN^{\text{ch}}}{dy}(b, y) = \int d^2s \frac{dN_{\text{NS}}^{\text{ch}}}{dy}(b, s, y) S_{\text{sh}}^{\text{ch}}(b, s, y). \quad (13)$$

At mid-rapidities, this quantity can be computed at various centralities using the coefficients $C_1(b)$ and $C_2(b)$ in Table 1 and (7). The calculations for AuAu collisions at mid-rapidities are shown in Fig. 1 and compared with experiment [15]. As predicted in [10] a reasonable description of the data is obtained. An increase by a factor 1.13 between $\sqrt{s} = 130$ GeV and $\sqrt{s} = 200$ GeV for central collision was also predicted in [10] – in agreement with the present data.

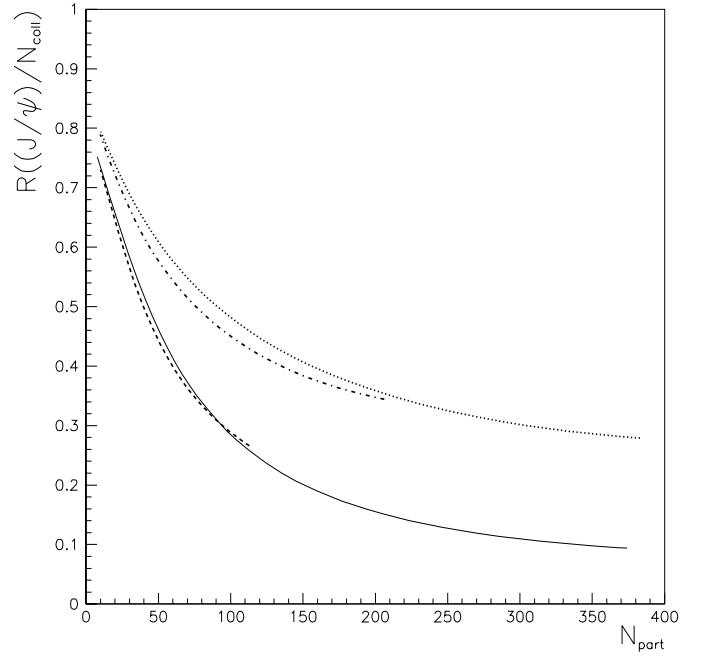


Fig. 2. $R_{AB}^{J/\psi}(b)$ for AuAu collisions at $\sqrt{s} = 200$ GeV (full curve), CuCu collisions at $\sqrt{s} = 200$ GeV (dashed curve), PbPb at $p_{\text{lab}} = 158$ GeV/c (dotted curve) and InIn at $p_{\text{lab}} = 158$ GeV/c (dashed-dotted curve). All the results have been obtained with $\sigma_{\text{co}} = 0.65$ mb and $\sigma_{\text{abs}} = 4.5$ mb. The normalization, the same for all four curves, is arbitrary. It corresponds to taking $dN_{pp}^{J/\psi}/dy = 1$ in (1)

In Fig. 2 we compare the result of our calculations of $R_{AB}^{J/\psi}(b)$ in (1) for different systems: PbPb² and InIn at CERN-SPS ($p_{\text{lab}} = 158$ GeV/c) and AuAu and CuCu at $\sqrt{s} = 200$ GeV. In all cases the normalization is arbitrary but the same for all. It corresponds to taking $dN_{pp}^{J/\psi}/dy = 1$ in (1). Also in all cases we use $\sigma_{\text{co}} = 0.65$ mb and $\sigma_{\text{abs}} = 4.5$ mb. An important feature of our results is that, at a given energy, the results for the lighter systems are rather close to the ones for the heavier ones, at the same values of N_{part} . We also see that the J/ψ suppression is much larger at RHIC energies and reaches a factor 10 for central AuAu collisions.

In Fig. 3 we present again the result of our calculation of $R_{\text{AuAu}}^{J/\psi}(b)$ in (1), with the normalization given by the measured value of $dN_{pp}^{J/\psi}/dy$ at $\sqrt{s} = 200$ GeV [16]. All curves are obtained with $\sigma_{\text{co}} = 0.65$ mb and different values of σ_{abs} ($\sigma_{\text{abs}} = 0, 1$ mb, 3 mb and 4.5 mb). The suppression for central collisions varies between a factor of 6 for $\sigma_{\text{abs}} = 0$ and a factor of 10 for $\sigma_{\text{abs}} = 4.5$ mb. Even in the former case the suppression is twice as large as the one obtained in a QCD based nuclear absorption model [17].

² The results for PbPb are identical to those in the first paper of [5], except that in [5] the ratio J/ψ over DY was plotted versus E_T (the energy deposited in the NA50 calorimeter). Moreover, for large E_T (beyond the “knee” of the E_T distribution) the effect of the fluctuation in the comovers' multiplicity was included. This is not the case in Fig. 2 since, in a plot versus N_{part} , such a situation does not arise.

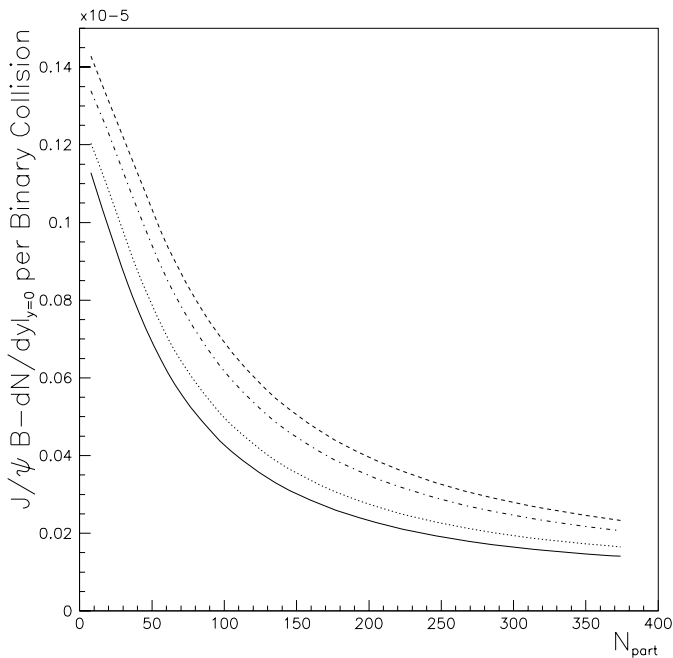


Fig. 3. $R_{AB}^{J/\psi}(b)$ for AuAu collisions at $\sqrt{s} = 200$ GeV multiplied by the dilepton branching ratio, normalized to the measured value in pp collisions [16]. From up to down: result with $\sigma_{co} = 0.65$ mb and $\sigma_{abs} = 0$ mb (dashed curve), result with $\sigma_{co} = 0.65$ mb and $\sigma_{abs} = 1$ mb (dotted-dashed curve), result with $\sigma_{co} = 0.65$ mb and $\sigma_{abs} = 3$ mb (dotted curve) and result with $\sigma_{co} = 0.65$ mb and $\sigma_{abs} = 4.5$ mb (full curve)

The results in Fig. 2 for PbPb and InIn has been obtained without including shadowing. Using (7) it turns out that, at CERN-SPS, the shadowing on the J/ψ is negligibly small. However, for the comovers ($m_T = 0.4$ GeV), its effect is of the order of 15%. Here the values of Y_{max} and Y_{min} in (8) are quite close to each other and our equations (and in particular the expression of Y_{min}) are not accurate enough for a reliable calculation. If, however, an effect of shadowing of the order of 15% is present, the values of C_1 and C_2 in Table 1 should be increased by the same amount in order to restore agreement [10] with the experimental values of the charged multiplicities in PbPb at $p_{lab} = 158$ GeV/c. This, in turn, would result in a larger J/ψ suppression at RHIC. The maximal effect occurs in the case $\sigma_{abs} = 0$ and is of the order of 20% for central AuAu collisions.

4 Conclusions

In a comovers' interaction framework we have computed the yield of J/ψ per binary nucleon–nucleon collision versus the number of participants in PbPb and InIn collisions at CERN-SPS ($p_{lab} = 158$ GeV/c) and in AuAu and CuCu at $\sqrt{s} = 200$ GeV. At RHIC energies shadowing corrections to both the J/ψ and the comovers' multiplicities are very important and have been included in the calculations. We have found that, at a given energy, the J/ψ suppression for the lighter and heavier systems are similar, at the same

value of N_{part} . We have also found that the J/ψ suppression at RHIC is significantly larger than at SPS. For central AuAu collisions it reaches a factor of 10 for $\sigma_{abs} = 4.5$ mb and a factor 6 for $\sigma_{abs} = 0$. The value of σ_{abs} has to be determined from the dAu data. Preliminary results [16] favor a rather small value, $\sigma_{ab} \approx 1$ mb.

We have argued that these values could be underestimated by about 20%. Experimental values of the J/ψ suppression significantly smaller than the one in Fig. 3 would not be consistent with the comovers' interaction model, at least in its present formulation.

Finally, an important difference between the J/ψ suppression pattern in a comovers' interaction model and in a deconfining scenario is that, in the former case, the anomalous suppression sets in smoothly from peripheral to central collisions – rather than in a sudden way when the deconfining threshold is reached. The NA50 results have not allowed one to disentangle these two possibilities. However, at RHIC energies, the relative contribution of the comovers is strongly enhanced in our approach, and a clear cut answer to this important issue should be obtained.

Acknowledgements. It is a pleasure to thank N. Armesto for interesting discussions and helpful suggestions. E. G. Ferreiro also thanks the Service de Physique Théorique, CEA, Saclay, for hospitality during the completion of this work.

References

1. M.A. Braun, C. Pajares, C.A. Salgado, N. Armesto, A. Capella, Nucl. Phys. B **509**, 357 (1998); M.A. Braun, A. Capella, Nucl. Phys. B **412**, 260 (1994); K. Borekov, A. Capella, A. Kaidalov, J. Tran Thanh Van, Phys. Rev. D **47**, 919 (1993)
2. B.Z. Kopeliovich, A.V. Tarasov, J. Huefner, Nucl. Phys. A **696**, 669 (2001)
3. NA50 Collaboration, L. Ramello, Nucl. Phys. A **715**, 243c (2003); L. Kluberg in Proceedings Quark Matter 2004, Oklahoma, USA
4. T. Matsui, H. Satz, Phys. Lett. B **178**, 416 (1986)
5. A. Capella, D. Sousa, Eur. Phys. J. C **30**, 117 (2003); A. Capella, D. Sousa, nucl-th/0110072; A. Capella, E.G. Ferreiro, A.B. Kaidalov, Phys. Rev. Lett. **85**, 2080 (2000); N. Armesto, A. Capella, E.G. Ferreiro, Phys. Rev. C **59**, 395 (1999); N. Armesto, A. Capella, Phys. Lett. B **430**, 30 (1998)
6. C.W. Jager et al., Atomic Data and Nuclear Tables **14**, 485 (1974)
7. B. Koch, U. Heinz, J. Pitsut, Phys. Lett. **243**, 149 (1990)
8. P. Braun-Munzinger, J. Stachel, Phys. Lett. B **490**, 196 (2000); R.L. Thews, M. Schrodtter, J. Rafelski, Phys. Rev. C **63**, 054905 (2001); A. Andronic, P. Braun-Munzinger, K. Redlich, J. Stachel, Phys. Lett. B **571**, 36 (2003); L. Grandchamp, R. Rapp, Nucl. Phys. A **709**, 415 (2002); A.P. Kostyuk, M.I. Gorenstein, H. Stoecker, W. Greiner, Phys. Rev. C **68**, 041902 (2003)
9. A. Capella, C-I. Tan, U. Sukhatme, J. Tran Thanh Van, Phys. Rep. **236**, 225 (1994)
10. A. Capella, D. Sousa, Phys. Lett. B **5111**, 185 (2001)

11. V.A. Abramovski, V.N. Gribov, O.V. Kancheli, Sov. J. Nucl. Phys. **18**, 308 (1974)
12. A. Capella, A. Kaidalov, J. Tran Thanh Van, Heavy Ion Phys. **9**, (1999)
13. N. Armesto, A. Capella, A.B. Kaidalov, J. Lopez-Albacete, C.A. Salgado, Eur. Phys. J. C **29**, 531 (2003)
14. PHENIX Collaboration, R. Granier de Cassagnac, nucl-ex/0403030
15. S.S. Adler et al., Phys. Rev. C **69**, 034909 (2004)
16. S.S. Adler et al., Phys. Rev. C **69**, 014901 (2004)
17. A.K. Chaudhuri, nucl-th/0307029